

See discussions, stats, and author profiles for this publication at: <https://www.researchgate.net/publication/260652508>

# Mathematical Modeling of Driver Speed Control With Individual Differences

Article in *IEEE Transactions on Systems Man and Cybernetics Systems* · September 2013

DOI: 10.1109/TSMC.2013.2256854

---

CITATIONS

36

---

READS

3,108

2 authors:



**Guozhen Zhao**

Chinese Academy of Sciences

60 PUBLICATIONS 1,498 CITATIONS

[SEE PROFILE](#)



**Changxu Wu**

State University of New York College at Buffalo

135 PUBLICATIONS 3,195 CITATIONS

[SEE PROFILE](#)

# Mathematical Modeling of Driver Speed Control With Individual Differences

Guozhen Zhao and Changxu Wu, *Member, IEEE*

**Abstract**—The quantitative prediction and understanding of a driver's speed control is an essential component in preventing speeding and designing of vehicle systems. Driver speed control is a complex behavior of longitudinal vehicle control consisting of speed perception, decision making, motor control, vehicle dynamics modeling, and individual driver differences. However, there are few existing models that can integrate all of these aspects in a cohesive manner. To address this problem, this paper introduces a mathematical model for a driver's speed control with analytical solutions based on human cognitive mechanisms in driving. This model includes an integrated queuing network-model human processor structure and the rule-based decision field theory. This new model consequently can predict several aspects of driver speed control behavior at the same time, such as driving speed, throttle/brake pedal angle, acceleration, and the frequency of speedometer inspection. A laboratory session involving a driving simulator is conducted to validate the current model. The model accounted for over 99% of the experimental speed of the average driver, and over 95% of the experimental speed for the majority of individual drivers.

**Index Terms**—Individual difference, mathematical model, queuing network, rule-based decision field theory, speed control

## I. INTRODUCTION

**D**RIVER'S SPEED control is a part of normal vehicle control, and consists of a series of time-sharing activities. A driver must constantly adjust or maintain his/her speed while simultaneously watching the road, checking the speedometer, and making critical decisions regarding speed choices. In order to support the quantitative analysis of such a complex behavior of a driver's speed control, it is important to develop computational models of human performance [1]. Computational models are not restricted to a specific aspect of human performance but attempt to model several aspects of it in a single, coherent, cognitive architecture [2].

### A. Existing Computational Models of Speed Control and Their Limitations

Two types of computational models have been developed to partially model a driver's speed control behavior:

Manuscript received November 30, 2011; revised June 3, 2012; accepted October 3, 2012. Date of publication August 1, 2013; date of current version August 14, 2013. This work was supported by the National Science Foundation. This paper was recommended by Associate Editor M. Mulder.

G. Zhao was with State University of New York at Buffalo, Buffalo, NY 14260 USA. He is now with the Chinese Academy of Sciences, Beijing 100864, China.

C. Wu is with State University of New York at Buffalo, Buffalo, NY 14260 USA (e-mail: changxu.wu@gmail.com).

Color versions of one or more of the figures in this paper are available online at <http://ieeexplore.ieee.org>.

Digital Object Identifier 10.1109/TSMC.2013.2256854

car-following and rule-based decision field theory (RDFT). Car-following models were by far the most widely extended acceleration models used for studying the mechanisms of vehicle speed control [3]. In the car-following model, the subject vehicle is assumed to follow a leading vehicle and maintain a safe distance from it. When this safe distance changes, the follower is assumed to apply the acceleration immediately. Later, general acceleration models that address non car-following situations were proposed [4], [5]. For example, Ahmed [5] developed a general acceleration model which applied to not only the car-following but also the free-flow regime. In the free-flow regime, a driver (follower) is not affected by the leader's behaviors (e.g., the leader's vehicle is far away from the driver), and the follower tries to attain his/her desired speed.

Another type of the computational modeling of a driver's decision making process in terms of speed choice is RDFT [6], an extension of Decision Field Theory (DFT) [7]. DFT provides a mathematical foundation that leads to a dynamic, stochastic theory of decision making when presented with an uncertain situation. RDFT builds upon DFT in order to accommodate multialternative preferences for each choice within a single theoretical framework, and also to allow for the application of multiple numbers of rules that become applicable in a specific environment. In this regard, RDFT has proven to be successful in previous applications that model a driver's cognitive behavior of speed choice [6].

Johnson and Busemeyer [6] proposed that there were multiple speed choices that describe different attributes in a repetitive decision making task. Such attribute information may consist of potential money lost (e.g., speeding ticket), time benefit (e.g., decreasing travel time), and safety consideration (e.g., potential accident). They further revealed that, when new drivers first begin to drive, they must deliberate over each speed choice presented to them on the first few occasions, using only attribute information. With repeated experience, most drivers begin to internalize a set of rules (e.g., decrease speed when snowing) that become applicable when deliberating over a target speed. As this set of rules develops for each driver as he/she gains more driving experience, his/her internalized rule(s) begin to compete with the primary attributes listed above depending on the driver's speed preference in any given situation.

Although two existing computational models have been used to model a driver's speed control, further examination of these models raises several questions that need to be addressed.

First, existing free-flow models assume that drivers are always aware of their traveling speed, which is impossible in reality. Recarte and Nunes [8] found that about 4% of the total number of eye fixations were focused on the dashboard. This indicated that a driver's eyes focused most of the time on external references outside of the car, and so the awareness of his/her traveling speed often tended to be based on subjective estimations.

Secondly, desired speed was expressed as a function of a heavy vehicle variable and a driver's characteristic variable in previous free-flow models [5]. In reality, however, setting a target speed involves complex and repetitive decision making processes. Specifically, speed choice involves a certain amount of information seeking, weighing of consequences, competition of multialternative attributes and/or rules, and conflict resolution. Therefore, previous free-flow models cannot fully explore the cognitive mechanism of speed choice.

Finally, existing free-flow models focused on the vehicle performance (such as vehicle acceleration or speed), while there were no model predictions offered for human behaviors (such as speed choice, foot movement time). These models assumed that drivers made instantaneous decisions regarding their desired speed and instantaneous foot movement for pedal operation, which is not a realistic model when studying driver speed control.

In contrast, RDFT has its unique advantage of fully exploring a driver's complex behavior of speed choice. As noted above, however, speed control consists of a series of activities, and decision making is only one component of the whole process. RDFT cannot model the process of how a driver perceives the speed or produces predictions with respect to the foot movement for pedal operation. Moreover, because RDFT does not include a vehicle mechanical model, it cannot quantify the relationship between pedal control and vehicle acceleration or overall speed. Finally, RDFT does not consider the effects of individual differences on a driver's speed control. As a result, another modeling technique, the queuing network-model human processor (QN-MHP), should be integrated with RDFT to serve as the basis to model a driver's complete speed control behavior.

### B. Queuing Network-Model Human Processor and Its Modeling of Driver Lateral Control

A computational cognitive model, QN-MHP, has been developed as a human psychological system to model and simulate human behaviors [2], [9]. Liu *et al.* [2] applied QN-MHP to model driver performance of lateral vehicle control, such as steering and lane keeping. In their study, there were two tasks involved: the primary task was to control a vehicle and keep it inside lane boundaries while the secondary task was to read a map in order to obtain the displayed information while steering a vehicle concurrently. Vehicle heading, lateral position, and road curvature served as model inputs, while driver's hand position (to move the steering wheel) and eye position were predicted. The model was tested and validated with a driving simulator.

Compared to RDFT, QN-MHP is a computational perceptual-motor model without complex decision making

involved. Therefore, the cognitive process of speed choice deals with multialternative speed decisions associated with different attributes/rules for specific driving conditions cannot be fully explained by QN-MHP. On the other hand, QN-MHP has its advantages to modeling not only the cognitive process of speed choice, but also speed perception and motor control. Moreover, QN-MHP has a unique mapping toward the brain areas which represent the mental architecture of information processing, and which in turn helps people understand the intrinsic mechanism of speed control in the mental system. In short, the integration of QN-MHP and RDFT is expected to quantitatively model the complete process of speed control including speed perception, complex cognitive process of decision making, and motor control.

### C. Research Objectives

Based on the results of existing research in this field, the objectives of this paper are to: 1) build a mathematical model with analytic solutions that quantify the mechanism of a driver's speed control; 2) integrate QN-MHP and RDFT to better explore the mechanism of the complete process of speed control, which includes speed perception, complex decision making, motor control, and a vehicle mechanical model; 3) model and predict the average driver's speed control behavior; and 4) model and predict individual differences of speed control resulting from individual decision making reference and impulsiveness.

## II. MODELING SPEED CONTROL WITH THE INTEGRATION OF QN-MHP AND RDFT

### A. Overview the QN-MHP Structure Involved in the Speed Control

In QN-MHP, brain regions with similar functions are represented as servers. Specific entities represent pieces of information that pass through and are processed by the servers. An entity travels on routes that represent neural pathways connecting the different brain regions. QN-MHP consists of perceptual, cognitive, and motor subnetworks. For a detailed description of the QN-MHP and each subnetwork, see [9].

As illustrated in Fig. 1, a few effective servers and routes in QN-MHP were used in the model presented in this paper. Visual inputs/entities (such as optical flow or posted speed limit information) enter the QN system at Server 1. These incoming entities are then transmitted in parallel pathways: one of which is routed to the visual recognition server (Server 2), which processes the content features (e.g., what is the current speed limit), and the other is routed to the visual location server (Server 3), where location features of entities (e.g., where is the current speed limit) are processed. These features from the two visual pathways are integrated at Server 4.

The cognitive subnetwork involves four servers. A visuospatial sketchpad represented by Server A integrates the individual pieces of feature information from the attended visual zone, and stores in working memory. Server F performs math calculation and complex decision making (e.g., set

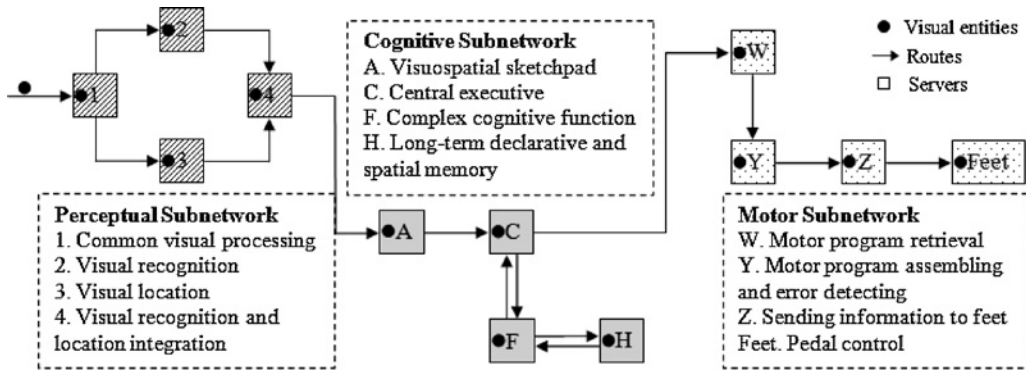


Fig. 1. Effective servers and routes in QN-MHP that were used in the model.

the target speed according to the current speed limit). The central executor represented by Server C communicates with Server F, and then transmits entities to the motor subnetwork. Server H represents declarative long-term memory and stores a set of attributes and rules derived from previous driving occasions.

The motor subnetwork contains five effective servers. When entities travel to the motor subnetwork, motor programs and long-term procedural information are retrieved (Server W) and assembled (Server Y). Then, the primary motor cortex (Server Z) decides the level of exerted force that can be converted to the level of pedal angular velocity. Then, the neural signals are transmitted from Server Z to the foot server, which executes foot movements for pedal operation. When the foot starts to move, Server X collects motor information from Server Z and sensory information (e.g., force feedback, muscle length, etc.) from the foot in real time, and then relays them to Server C as well as Server Y.

**B. Integration of QN-MHP and RDFT**

In this model, the original QN-MHP was integrated with RDFT to fully explore the complete mechanism of a driver’s speed control. According to the QN-MHP, Server F in the cognitive subnetwork (Fig. 1) performed complex cognitive functions such as multiple-choice decision, visuomotor choices, anticipation of stimuli in simple reaction tasks, etc. Thus, it was possible that the deliberation process in RDFT was incorporated in this Server F. Also, the deliberation time within a single choice in RDFT was assumed to be equal to one processing cycle time in Server F (18ms on average). In addition, as driving experience increases, a set of rules and attributes derived and modified during previous driving occasions might be stored in Server H (declarative long-term memory) in the cognitive sub-network. This server stored various production rules in choice reaction, long-term spatial information, perceptual judgment, decision making, and problem solving. When a driver is making a decision on his/her speed, Server F could communicate with Server H and look for either the attributes or rules that become applicable for that specific driving condition. Finally, the attributes or rules stored in Server H could be modified or updated. By integrating with RDFT, the original QN-MHP was

enhanced and used as a basis to explore the mechanism of speed control.

**C. Mathematical Modeling of Speed Control in the Integrated QN-MHP**

The desired new model outlined above involves five major components: 1) speed perception; 2) decision making; 3) motor control; 4) a vehicle mechanical model; and 5) individual differences.

1) *Speed Perception Component:* Most of the time, in a real driving situation, drivers are aware of their traveling speed relying on perceptual cues, combined with occasional speedometer inspection. These perceptual cues may be visual, auditory, or kinesthetic cues. While each category plays an important role in assessing traveling speed, visual cues (e.g., optical flow), serve as the predominant reference that drivers use to estimate their traveling speed [10].

Optical flow refers to the relative velocity of points across the visual field as we move through the world. Owen *et al.* [11] identified two aspects of the optic array that may affect the perception of egospeed: global optical flow rate and optical edge rate. Global optical flow rate ( $\Phi\#$ ) is defined as the velocity of forward motion scaled in unit of altitude or eye height per second. It varies directly with driving speed ( $V$ ) and inversely with altitude ( $H$ ). Another source of information for perceiving egospeed is discontinuity rate or optical edge rate. Optical edge rate ( $\Delta$ ) is defined as the rate at which local discontinuities cross a fixed point of reference in the observer’s field of view. Velocity, in edges per second, can be calculated by timing how many edges pass a reference point per second. It varies directly with the density of visible texture ( $D$ ) and speed ( $V$ ).

In most real world situations, global optical flow and edge rate are correlated and contribute additively to perception of self-motion [12]. According to [13] work, as well as the effects of actual speed and eye height (altitude) on the perceived optical flow revealed in the literature, we proposed that the ratio of perceived speed to actual speed ( $V$ ) directly varied with the ratio of the current texture density ( $D_c$ ) to the texture density in the last driving scenario ( $D_l$ ), and the ratio of the eye height in the last driving scenario ( $H_l$ ) to the current eye height ( $H_c$ ) [see (1)], with two constant parameters  $k_1$  and  $k_2$ . Here, drivers were assumed to check the speedometer and be

aware of their traveling speed accurately in the last driving scenario

$$v_p = \left(\frac{D_c}{D_l}\right)^{k_1} \times \left(\frac{H_l}{H_c}\right)^{k_2} \times V. \quad (1)$$

The parameter  $k_1$  was estimated to be between 0.118 and 0.123 in previous experimental studies [12], [13]. If context or objects (such as poles) are evenly distributed, the ratio of context density is inversely proportional to the ratio of the space ( $L$ ) between two contiguous objects

$$\frac{D_c}{D_l} = \frac{L_l}{L_c}. \quad (2)$$

When a driver visually checks the speedometer, his/her perceived speed is equal to the actual vehicle speed

$$v_p = V. \quad (3)$$

According to the processing logic of QN-MHP, Server 3 in the perceptual subnetwork processes the information related to the object location features (such as speed). Thus, the three math equations proposed above can be implemented in this server.

The frequency of speedometer inspection was described as the ratio of the total time duration of eye fixation on the speedometer, which is expressed by the total driving time ( $T_t$ ) multiplying the percentage of fixation on the speedometer ( $p$ ) to the average time duration of fixation on the speedometer at one time ( $\bar{T}_s$ ) [see (4)]. Recarte and Nunes [8] reported that around 4% of the eye fixations were performed on the dashboard during ordinary driving without the effect of other tasks. In addition,  $\bar{T}_s$  was estimated to be between 760 and 880 ms [14]

$$[f] = \frac{T_t \times p}{\bar{T}_s}. \quad (4)$$

2) *Decision Making Component*: RDFT introduces two levels of dynamics: The deliberation process with a single choice and the learning process based on the outcomes across choices [6]. In normal driving conditions, a driver is assumed to make a decision on his/her target speed only based on the attributes associated with each speed choice. Rules that are derived from previous driving occasions for specific driving conditions (such as bad weather condition, heavy traffic flow, etc.) are stored in the human mental system, but are not applicable in such normal driving conditions. Johnson and Busemeyer [6] formulated a metric  $M$  for the possible outcome to demonstrate the cognitive process of speed choice. The current model used a similar method to construct a subjective attribute matrix for each driver (see Section II.C.5.a in detail).

RDFT assumes that, at each point in time during deliberation, the attention weights  $W(t)$  select only a single attribute  $j$ , which focuses on the values of a single attribute from  $M$  [i.e.,  $W_j(t) = 1$ ,  $W_k(t) = 0$ , for all  $k \neq j$ ]. This model used the same method to assign the attention weight for average drivers or normal drivers. However, considering the potential effects of impulsiveness, the attention weights for either impulsive or non-impulsive drivers were different (see Section II-C5.2 in details).

The momentary valence  $V(t)$  is the advantage of an alternative relative to all others on this processed attribute (see (5), [15]). The default form of the contrast matrix  $C$  that performs this comparison is such that the diagonal elements  $C_{xx} = 1$ , and the off-diagonal elements  $C_{xy} = -1/(m-1)$ , where  $m$  is the number of alternatives. Adding this valence to some degraded trace (by  $S$ ) of the previous preference state results in the momentary preference vector  $P(t)$ , containing (as elements) the preference values for all alternatives (see [15, eq. (6)]). For a detailed description of parameters estimation, see Appendix A

$$V(t) = C \times M(n) \times W(t) \quad (5)$$

$$P(t) = S \times P(t-1) + V(t). \quad (6)$$

To determine when a choice is made, a threshold parameter  $\theta$  is used for terminating this deliberation process. In other words, a decision maker must determine at some point that he/she has deliberated enough and a decision should be made. In this model, the preference for each speed choice accumulates over time. If any preference for its associated speed choice  $P(t)$  exceeded the decision threshold  $\theta$ , such speed choice was selected and no further deliberative process is assumed. Then, the target speed  $v_{tar}^*(t)$  at time  $t$  was decided by adding both selected speed choice  $v_{P_i(t) \geq \theta}$  and the speed limit  $V_{sl}$

$$v_{tar}^*(t) = V_{sl} + v_{P_i(t) \geq \theta}. \quad (7)$$

Besides attributes, the proposed speed control model was able to examine the influence of rules on a driver's behavior of speed choice. In particular, each rule could be represented by a column in the rule matrix  $X$  providing advice favoring one alternative over other alternatives. In general, attributes and rules formulate a concatenated matrix  $[M|X]$ . If a specific condition is present, then one of the columns of the rule is selected for advice. For example, if it is snowy, a driver may refer to the rule of bad weather (the first column) in the rule matrix  $X = [\theta \ 0 \ 0 \ 0]^T$ . Since the value for the first option (follow the speed limit) is sufficiently strong enough to terminate the deliberation process, the first choice is immediately selected.

Based on the processing logic of the QN-MHP and the route of speed control defined in Fig. 1, the expected reaction time (starting from perceiving the information of the speed limit, and ending in transmitting neural signals from the primary motor cortex to the foot server) was estimated by adding the processing time for all effective servers together (see (8), [9], [16]). The subscript letter "P" stands for the perceptual subnetwork and other letters are associated with corresponding servers in QN-MHP, respectively

$$\tau = T_P + T_A + T_C + T_F + T_H + T_F + T_C + T_W + T_Y + T_Z \quad (8)$$

3) *Motor Control Component*: Upon realizing the difference between his/her own desired target speed and perceived speed, the driver reacts by moving the feet accordingly in order to operate the pedal. Let  $\theta_0$  be the steady state of the vehicle pedal input. Define  $d\theta = \theta - \theta_0$  as the deviation of the pedal angle from  $\theta_0$ . Based on the QN-MPH, when

neural signals are transmitted from the primary motor cortex (Server Z) to the foot, the associated muscles' elements produce force to execute foot movements for pedal operation. Because this proposed model provides predictions every 100ms, it is assumed that the pedal moves with constant acceleration during each short time interval. Accordingly, we proposed that pedal angular velocity ( $\omega$ ) directly varied with the difference between target speed ( $v_{tar}^*$ ) and perceived speed ( $v_p$ ), with a constant parameter  $A$

$$\omega = \frac{d\theta}{dt} = A \times (v_{tar}^* - v_p). \quad (9)$$

Foot movement for pedal control, in general, is carried out without visual guidance [17], [18]. Unlike an emergency, where drivers must act as quickly as possible to avoid traffic accidents, a driver's speed control, as a normal driving task, does not require any urgent pedal control. Thus, drivers are assumed to not move their feet beyond a comfortable range for the ankle (e.g., 80–113°, [19]). Here, the angle of the ankle refers to the angle between a line from the lateral condyle to the lateral malleolus and a line parallel with the foot. This assumption is explained by the feedback control mechanism in the body's central nervous system: when the foot rotates around the heel joint, the muscle-spindles sense changes in muscle stretch velocity and Golgi tendon organs detect changes in muscle force.

Foot switching time ( $t_b$  in ms) is the time a driver moves his/her foot from one pedal to the other. Hoffmann [20] described the foot movement time between two pedals as a function of a lateral separation of both pedals ( $A_l$ ) and a perpendicular separation of both pedals ( $A_{pe}$ ) [see (10)]. It was assumed that the foot lifted about 50mm when a driver switched from the accelerator to the brake in order to prevent interference, and thus the effective vertical displacement of the pedal was approximated by  $A_{pe} = A_p + 50$

$$t_b = 123 + \frac{61.1 \times (A_{pe} + 11.6)}{A_l} + \frac{124.3 \times (A_l - 17.2)}{A_{pe}}. \quad (10)$$

4) *Vehicle Mechanical Model*: Foot movement leads to the changes of pedal inputs, causing the following changes of vehicle acceleration and speed. Previous vehicle mechanical models as well as experimental studies have shown that the vehicle speed is a nonlinear function of the throttle angle. For example, Ioannou and Xu [21] proposed that the vehicle speed varied as a function of the throttle angle, time period and the presence of dynamics during an acceleration process. Similarly, during a deceleration process, the vehicle speed varied with the braking force, the static friction force, air resistant force, etc. In order to simplify this mechanical process, we proposed a simple linear equation to approximately quantify the relation between the deviation of pedal input and the deviation of acceleration. As illustrated in (11), at each short time interval  $\Delta t$ , the deviation of the acceleration ( $da$ ) directly changes with the deviation of the pedal angle ( $d\theta$ ), and  $B$  is a constant parameter estimated in a previous experimental study [22]

$$da = B \times d\theta. \quad (11)$$

Then, the acceleration applied at the next time interval  $\Delta t$  was described as follows:

$$a = a_0 + da - c_g \times V^2 \quad (12)$$

where  $a_0$  and  $c_g$  represented the initial acceleration and the coefficient of the overall drag on the vehicle ( $c_g$  is set by the driving simulator). The overall drag of the vehicle increases with the square of the vehicle speed. At some point, it will balance with the vehicle's acceleration and vehicle's speed will no longer increase. Therefore, this overall drag of the vehicle determines the vehicle maximum speed in this driving simulator. This parameter also affects how fast the vehicle decelerates when coasting. The higher the drag coefficient the faster the vehicle will decelerate during coasting. Finally, (13) expresses the vehicle's speed at the next time interval as  $\Delta t$ . For parameters used in the vehicle mechanical model, Appendix B gives a detailed description

$$V = V_0 + a\Delta t. \quad (13)$$

5) *Individual Differences*: In this paper, we modeled two individual differences: individual decision making references and impulsiveness.

Individual driver differences in a decision making reference Each driver has his/her own decision making reference that is derived and modified during previous driving instances. The National Highway Traffic Safety Administration (NHTSA) reported that drivers, on average, believe that they can drive about 7–8 mi/h over the posted speed before they will be ticketed [23]. Such speed references may be affected by many environmental factors, such as the speed limit, road type, weather condition, traffic flow, and social environmental variables, such as surrounding drivers [24].

A subjective attribute matrix  $M$  was constructed for each driver. Each row represents an option or speed choice and each column depicts a possible outcome. The numbers at the cross-section of each row and column are subjective values that each individual driver associates with the cost/benefit of speeding. Because these numbers are the aggregation of multiple attributes (monetary cost of receiving a speeding ticket, a gain in terms of safety, and saving travel time), no qualifying units are assigned to these values (i.e., no unit of measurement). Every driver established their own individual reference points including the number of rows and columns, scales, and the values in each cell. For example, as shown in Table I, there are four speed choices: 1) follow the speed limit (no speeding); 2) drive over the speed limit at 5 mi/h (drive at +5); 3) drive over the speed limit at 10 mi/h (drive at +10); 4) and drive over the speed limit at or greater than 15 mi/h (drive at  $\geq +15$ ). Also, there are four possible outcomes: driver gets a speeding ticket when driving 5 mi/h over the speed limit (Ticket at +5), 10 mi/h (Ticket at +10), or at 15 mi/h (Ticket at  $\geq +15$ ), or driver receives no speeding ticket no matter how fast he/she drives (No ticket). If the driver drove over the speed limit by 5 mi/h and got caught (the case at the cross-section of the second row and the first column in Table I), the driver feels that he/she would experience a net loss of  $-300$  from receiving a ticket even if he/she gains some time and safety benefits. Based

TABLE I  
SUBJECTIVE VALUES IN TERMS OF MONETARY COST, A GAIN OF TIME,  
AND SAFETY (FURTHER DEVELOPED FROM [6])

	Ticket at +5 mi/h	Ticket at +10 mi/h	$\geq +15$ mi/h	No ticket at all
No speeding	100	100	100	100
Drive at +5 mi/h	-300	250	250	250
Drive at +10 mi/h	-250	-300	500	500
Drive at $\geq +15$ mi/h	-500	-300	-300	750

on this attribute matrix, each driver's desired target speed was calculated. For a detailed description of the mathematical deduction and parameter settings, see Appendix A.

Individual driver differences in impulsiveness with its effects on decision making and motor control Impulsiveness is a salient factor that has received attention in literature on accident prevention. Impulsiveness is one component of risk-taking, and it is associated with driving anger [25] and the most aggressive driving, such as speeding [26]. It deals with a person's control over his/her thoughts and behavior, which may lead to speeding behavior if an individual lacks the self-control to refrain from engaging in such an action [27]. In this paper, we focus on modeling the effects of impulsiveness on decision making and motor control since previous empirical studies have not shown evidence on the influence of impulsiveness on speed perception.

Compared to normal drivers, those who are characterized as impulsive or non-impulsive drivers may have strong preferences for attending to a specific attribute. While these drivers are determining about how fast to drive, their attention may shift to thinking about each possible outcome (the police ticket at +5, +10,  $\geq +15$  mi/h, or not at all), rather than stochastically drifting from one attribute to another in which the probability of attention to an attribute at each moment is equal to the probability (of occurrence) of each outcome [6]. Accordingly, we proposed another way to form the attention weights matrix  $W(t)$  to represent how impulsive or non-impulsive drivers shift their attention (the possibilities of the occurrence) for each outcome. More specifically, the Extroversion (E) and Neuroticism (N) scales of Eysenck's personality system [28], [29] were used to divide all drivers into three categories: normal drivers (those characterized as  $E^+$  and  $N^-$  or  $E^-$  and  $N^+$ ); impulsive drivers (those characterized as  $E^+$  and  $N^+$ ); and non-impulsive drivers (those characterized as  $E^-$  and  $N^-$ ). Then, normalized scores<sup>1</sup> (ranging from 0 to 1) in E and N scales of Eysenck's personality system were averaged (represented by  $\bar{x}$ ). For impulsive drivers,  $\bar{x}$  represents the probability of attending to the time benefit, and the remainder from one is evenly distributed among the alternatives. By contrast,  $(1 - \bar{x})$  represents the probability of attending to the speeding cost and driving safety, and  $\bar{x}$  is evenly distributed among the alternatives for nonimpulsive drivers.

<sup>1</sup>For example, in a short form of the Revised Eysenck Personality Questionnaire (EPQR-S), Extroversion and Neuroticism each scale contains 12 items (ranging from -12 to 12). Normalized scores  $x' = x/24 + 0.5$  ( $x$ : original scores in E and N scales;  $x'$ : normalized scores in E and N scales).

Secondly, personality effects on motor speed control have been well established in a variety of tasks (e.g., circle tracing task, [30]–[32]). Of the variety of personality inventories available, the relations between motor speed and personality are mostly consistent for E and N scales of Eysenck's personality system with a variety of behavioral paradigms [33]. Bachorowski and Newman [30] reported that impulsive persons (characterized as  $E^+$  and  $N^+$ ) have faster motor speed in a task calling for slow and controlled movement compared to non-impulsive ones (low scores on both scales), and that this effect was more salient when a behavioral goal was present. As illustrated by (14), a personality characteristic variable ( $\eta$ ) which represents the degree of impulsivity or the tendency to act rapidly without deliberation [34] was introduced in (9). Based on Bachorowski and Newman's findings in their previous study,  $\eta$  was estimated accordingly (0.736 for drivers characterized as  $E^-$  and  $N^-$ ; 1.533 for  $E^+$  and  $N^+$ ; and 1 for  $E^+$  and  $N^-$  or  $E^-$  and  $N^+$ )

$$\omega = \frac{d\theta}{dt} = A \times \eta \times (v_{tar}^* - v_p). \quad (14)$$

#### D. Assumptions

In this paper, several assumptions were made to facilitate the development of the model. First, this model focused on a driver's speed control behavior in a free-flow traffic condition. Free-flow refers to a driver's speed control behavior as voluntary and unaffected by upstream or downstream driving conditions [35]. It is critical in capacity analysis procedures for basic freeway segments and multilane highways, and traffic stream analysis for incidents and bottlenecks [35]. Free-flow occurs in real driving conditions where there are no other vehicles involved, or there are other vehicles but they do not influence a driver's speed control behavior. In this paper, a driver was assumed to change his/her speed only when the speed limits change. Secondly, we integrated speed perception, decision making, motor control, vehicle mechanics, and individual differences to model a driver's speed control behavior. If any one of these five components is missing (i.e., a driver may not perceive his/her traveling speed while distracted), the model cannot provide predictions with regards to several components involved in driving.

### III. AN EXPERIMENTAL STUDY TO VALIDATE THE MODEL'S PREDICTION

A laboratory session involving a driving simulator was conducted to validate the mathematical model of driver speed control.

#### A. Participants

Twelve participants (6 males, 6 females) ranging from age 26 to 50 ( $M=34.5$ ,  $SD=5.58$ ) took part in this paper. Their average driving experience was 4.76 years and average annual mileage was 9200 miles. All of them had valid driver licenses, at least three years of driving experience, and had driven within the past month.

### B. Self-Report Measures

All participants were asked to complete a set of questionnaires after engaging in the driving task. The first questionnaire was designed to capture the participant's demographics (such as age and gender) and driving history (such as estimated cumulative driving mileage, the year a driver license was first issued, etc). Then, they were required to construct a subjective value matrix (reference Table I). Associated with each speed option was a monetary cost of receiving a speeding ticket and gain in terms of safety and time if no ticket was received. The value in each cell represented a driver's thoughts on the cost/benefit tradeoffs for each speed choice. Finally, a short form of the Revised Eysenck Personality Questionnaire (EPQR-S, [29]) was used to divide all drivers into three categories: normal drivers (those characterized as  $E^+$  and  $N^-$  or  $E^-$  and  $N^+$ ,  $n=6$ ); impulsive drivers (those characterized as  $E^+$  and  $N^+$ ,  $n=3$ ); and non-impulsive drivers (those characterized as  $E^-$  and  $N^-$ ,  $n=3$ ).

### C. Apparatus

A STISIM driving simulator (STISIMDRIVE M100K) was used in the study. It includes a Logitech Momo steering wheel with force feedback, a throttle pedal, and a brake pedal. The STISIM simulator was installed on a Dell Workstation (Precision 490, Dual Core Intel Xeon Processor 5130 2GHz) with a 256 MB PCIe  $\times$  16 nVidia graphic card, Sound Blaster X-Fi $\&$ trade; system, and Dell A225 Stereo System.

### D. Driving Scenario

The test block was a simulated two-lane (in each direction) highway environment. There were no pedestrians, traffic lights, or road signs (e.g., stop/yield signs) involved. There were other vehicles that randomly appeared in front of the driver's vehicle. However, all of them were very far away ( $\geq 150$  m) so that the driver's speed control behavior would not be affected by other vehicles. Speed limit signs with three levels of speed limits (25, 45, and 65 mi/h) were displayed 60 m in front of the driver. Participants were instructed to adjust their speed as if they were driving a real vehicle on the road. In addition, context density was kept constant throughout the entire test block.

### E. Experimental Design and Procedures

Two independent variables (acceleration versus deceleration; speed limit changes 20 mi/h versus speed limit changes 40 mi/h) were examined in the current session, resulting in four combinations: acceleration from 25 mi/h and maintain at 45 mi/h; acceleration from 25 mi/h and maintain at 65 mi/h; deceleration from 65 mi/h and maintain at 45 mi/h; deceleration from 65 mi/h and maintain at 25 mi/h. Another acceleration process 25–45 mi/h and deceleration process 45–25 mi/h were assumed to be similar to 45–65 mi/h and 65–45 mi/h, so these two conditions were not considered. Each acceleration or deceleration process was repeated twice in each trial.

Upon arrival, all participants were first asked to sign a consent document. After completing a set of questionnaires, all participants went through a practice session that allowed

them to get familiar with the driving simulator control. The practice session lasted one half hour and contained all features that appeared in the test blocks. Before the formal experiment, participants were allowed to adjust the seat so that they felt comfortable. There were two trials in the test block session. Each trial (20 km) lasted for 15–20 min depending on individual driving speed. Participants were allowed to take a 5-min brake between trials and were compensated for their time (\$10 per hour).

### F. Measurement

Behavioral measures from the driving simulator test block were automatically collected: time elapsed (in seconds), speed (in m/s), acceleration (in  $m/s^2$ ), gas pedal angle (in degrees), and brake pedal angle (in degrees). No drivers applied the brake pedal during an acceleration process, so the measurement of brake pedal angle was only applicable in a deceleration process. The frequency of eye fixation on the speedometer was measured by a video recording system. These experimental driving data were compared with modeled ones. The comparisons made are discussed in the following section.

## IV. VALIDATION OF MODEL PREDICTIONS WITH EXPERIMENTAL DATA

Given the mathematical equations introduced above and parameter estimations, the current model was able to predict a driver's speed control behavior. It is worth noting that there are no free parameters in this model. A free parameter is the parameter adjusted to fit the simulation results with the experimental data. Each free parameter, in general, can be regarded as a task-specific assumption [9]. Accordingly, the fewer number of free parameters there are, the fewer number of assumptions needed and the better the generalization the model can maintain. Parameter settings in the current model were provided in Appendix C.

The model was validated by comparing model predictions with experimental data. In the first step, modeled average speed, pedal angle, and acceleration were compared with averaged experimental data across drivers and trials (12 drivers  $\times$  2 trials  $\times$  2 replications in each trial), regardless of the effects of individual factors. Next, the influence of individual decision making references and the influence of impulsiveness were considered, respectively. Finally, both individual factors were considered at the same time. Note that from steps 2 to 4, modeled speed, pedal angle, and acceleration combined all drivers' individual data to make a single prediction. In addition, modeled average speed for each driver was compared with his/her experimental speed data, taking into account the effects of both individual factors. Due to page limits, only one acceleration process (25–65 mi/h) and one deceleration process (65–25 mi/h) were validated from steps 2 to 5. Finally, the frequency of speedometer inspection was also modeled.

Although each acceleration/deceleration process lasted for 2–3 min, we only truncated and displayed a 30 s time window for each process. After this 30 s window, based on our experimental data, drivers maintained a constant speed until the next speed limit appeared. The starting point of each

TABLE II  
 $R^2$  AND RMS FOR MODEL PREDICTIONS WITHOUT THE EFFECTS OF  
 INDIVIDUAL FACTORS

	$R^2$	RMS
Accelerated from 45 mi/h and maintained at 65 mi/h		
Gas pedal angle ( $^\circ$ )	0.899	0.78
Acceleration ( $\text{m/s}^2$ )	0.914	0.14
Speed (m/s)	0.801	1.25
Accelerated from 25 mi/h and maintained at 65 mi/h		
Gas pedal angle ( $^\circ$ )	0.8	1.75
Acceleration ( $\text{m/s}^2$ )	0.811	0.33
Speed (m/s)	0.96	1.15
Decelerated from 65 mi/h and maintained at 45 mi/h		
Gas pedal angle ( $^\circ$ )	0.684	1.21
Acceleration ( $\text{m/s}^2$ )	0.893	0.17
Speed (m/s)	0.975	0.33
Brake pedal angle ( $^\circ$ )	0.779	2.42
Decelerated from 65 mi/h and maintained at 25 mi/h		
Gas pedal angle ( $^\circ$ )	0.731	0.81
Acceleration ( $\text{m/s}^2$ )	0.908	0.26
Speed (m/s)	0.958	1.17
Brake pedal angle ( $^\circ$ )	0.858	4.55

30 s time window was the time when the driver was within 200 ft of each speed limit sign. For each step,  $R^2$  results and root mean square (RMS) results were provided to indicate how well the experimental data could be explained by the model. Nonparametric (Paired Samples) tests were performed to examine the differences between model predictions and experimental data at an alpha level of 0.05.

#### A. Model Average Speed Without Individual Differences

Modeled speed, pedal angle, and acceleration for the average driver were compared to the averaged experimental data (Fig. 2). The corresponding  $R^2$  and RMS are provided in Table II. Without the effects of individual differences, the model was able to account for roughly 95.8–97.5% of the experimental data in terms of speed during two deceleration processes and one acceleration process (25–65 mi/h). Although a much lower value of  $R^2$  was derived compared to the one for the other three conditions, the model was able to account for 80.1% of the experimental speed when drivers accelerated from 45 mi/h and eventually maintained 65 mi/h, which was still acceptable. In terms of RMS, on the other hand, one deceleration process from 65 to 25 mi/h had a smaller magnitude of variations for speed (around 0.32 m/s), whereas the magnitude was 1.15–1.25 m/s for the other three driving conditions.

#### B. Model Average Speed Considering Individual Differences in Decision Making Reference

A subjective value matrix in RDFT was used for each driver to model his/her speed choice and the speed control behavior. After considering individual decision making references, experimental data were better predicted by the model for both acceleration and deceleration processes: overall  $R^2$  and RMS improved by 8.3 and 32.9%, respectively (Table III). Specifically,  $R^2$  for experimental speed enhanced from 0.96 to 0.984 by 2.5%, and RMS decreased by 32.2% (from 1.15 to

0.78 m/s) during the acceleration process (25–65 mi/h).  $R^2$  for experimental speed improved from 0.958 to 0.986 by 2.9%, and RMS reduced by 45.3% (from 1.17 to 0.64 m/s) in the deceleration process (65–25 mi/h).

#### C. Model Average Speed Considering Individual Differences in Impulsiveness

The factor associated with personality changed its values for those drivers characterized as either impulsive or non-impulsive individuals. Compared to the decision making reference, impulsiveness did affect a driver's speed control behavior but not as much as the individual decision making reference: overall  $R^2$  and RMS improved by 5.6 and 17.4%, respectively (see Table III). Specifically,  $R^2$  for experimental speed increased from 0.96 to 0.976 by 1.7% and RMS decreased by 11.3% (from 1.15 to 1.02 m/s) during the acceleration process (25–65 mi/h).  $R^2$  for experimental speed enhanced from 0.958 to 0.964 by 0.6%, and RMS decreased by 5.1% (from 1.17 to 1.11 m/s) during the deceleration process (65–25 mi/h).

#### D. Model Average Speed Considering Individual Differences in Decision Making Reference and Impulsiveness

When we considered the effects of both individual factors, the model was able to explain around 99% of the experimental speed for both acceleration and deceleration processes (Table III). Overall,  $R^2$  and RMS improved by 9.3 and 41.5%, respectively. In particular,  $R^2$  for the experimental speed improved by 3.1% (from 0.96 to 0.99) during the acceleration condition (25–65 mi/h), and 3.7% (from 0.958 to 0.993) during the deceleration condition (65–25 mi/h). RMS for experimental speed also improved by 47% (from 1.15 to 0.61 m/s) in the same acceleration process and 60.7% (from 1.17 to 0.46 m/s) in the same deceleration process.

#### E. Model Individual Speed Considering Individual Differences in Decision Making Reference and Impulsiveness

At this step, modeled speed for the individual driver was compared to his/her experimental speed. Due to page limits, we only provided the 1st, 2nd, and 3rd 4-quantiles for driving speed based on  $R^2$  results in ascending order (Fig. 3). Overall, the model was able to explain 94.5–99.7% of the experimental speed (magnitude of variation: 0.37–1.57 m/s) for the majority of drivers. For driver 5 (65–25 mi/h) and driver 8 (25–65 mi/h), the model could explain 70.9% and 76.1% of the experimental speed with a larger magnitude of variations for speed (magnitude of variation: 2.78–3.11 m/s) (see Table IV).

#### F. Model the Frequency of Speedometer Inspection

Mourant and Rockwell [14] reported that experienced drivers (who had driven at least 8000 miles a year for the last 5 years), on average, spent 760 ms on each speedometer checking. In this experiment, participants had similar driving experience, so we used 760 ms as the average time duration of each fixation on the speedometer ( $\bar{T}_s = 0.76$ ). During a 30 s time period, the number of eye fixations on the speedometer was approximately modeled as being equal to 2. Experimental results showed that the average number of eye fixations on the speedometer was 2.15 (SD=0.99) when drivers accelerated

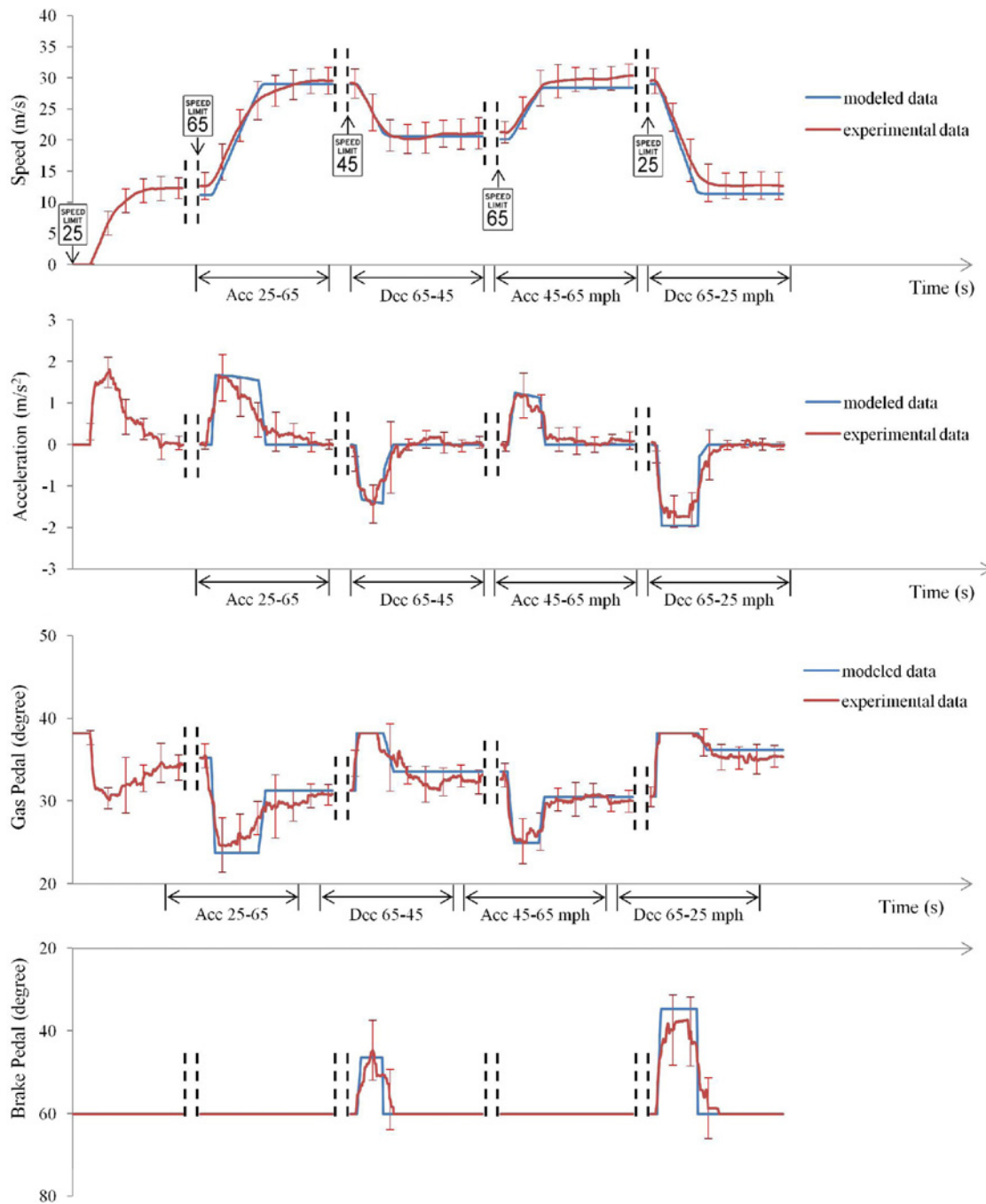


Fig. 2. Comparisons of modeled speed, pedal angle and acceleration for the average driver with averaged experimental data (error bars represent  $\pm 1$  standard deviation of experimental data).

from 25 to 65 mi/h. The percentage of relative error (estimation error, [36]–[38])<sup>2</sup> was 7.1%. The Mann–Whitney Test did not reveal significant differences between modeled and experimental results ( $U = 78, Z = -0.39, p = 0.78$ ). During a deceleration process (65–25 mi/h), the average number of eye fixations on the speedometer was 2.4 (SD = 1.12, estimation error = 16.1%) and there was no significant difference between modeled and experimental data ( $U = 71.5, Z = -0.82, p = 0.36$ ).

<sup>2</sup>The estimation error is derived based on  $|Y - X|/X \cdot 100\%$ .  $Y$ : modeled result;  $X$ : experimental result.

## V. DISCUSSION

This paper introduces a mathematical model for a driver’s speed control with analytical solutions based on a rigorous understanding of the human cognitive mechanisms involved in driving. This model integrates the QN-MHP with RDFS to explore the complete mechanism of a driver’s speed control by unifying speed perception, decision making, motor control, vehicle dynamics modeling, and individual differences. A laboratory session involving a driving simulator was conducted to validate the current model. Considering

TABLE III  
 $R^2$  AND RMS FOR MODEL PREDICTIONS WITH THE EFFECTS OF INDIVIDUAL FACTORS

	$R^2$	$R^2$ improved (%)	RMS	RMS improved (%)
1. Consider individual differences in decision making references				
Accelerated from 25 mi/h and maintained at 65 mi/h				
Gas pedal angle (°)	0.848	6	1.42	18.9
Acceleration (m/s <sup>2</sup> )	0.876	8	0.24	27.3
Speed (m/s)	0.984	2.5	0.78	32.2
Decelerated from 65 mi/h and maintained at 25 mi/h				
Gas pedal angle (°)	0.92	25.9	0.48	40.7
Acceleration (m/s <sup>2</sup> )	0.951	4.7	0.18	30.8
Speed (m/s)	0.986	2.9	0.64	45.3
Brake pedal angle (°)	0.925	7.8	2.95	35.2
Average of the percentage of improved $R^2$ and RMS		8.3		32.9
2. Consider individual differences in impulsiveness				
Accelerated from 25 mi/h and maintained at 65 mi/h				
Gas pedal angle (°)	0.832	4	1.41	19.4
Acceleration (m/s <sup>2</sup> )	0.873	7.6	0.24	27.3
Speed (m/s)	0.976	1.7	1.02	11.3
Decelerated from 65 mi/h and maintained at 25 mi/h				
Gas pedal angle (°)	0.867	18.6	0.65	19.8
Acceleration (m/s <sup>2</sup> )	0.922	1.5	0.23	11.5
Speed (m/s)	0.964	0.6	1.11	5.1
Brake pedal angle (°)	0.903	5.2	3.291	27.7
Average of the percentage of improved $R^2$ and RMS		5.6		17.4
3. Consider individual differences in both decision making references and impulsiveness				
Accelerated from 25 mi/h and maintained at 65 mi/h				
Gas pedal angle (°)	0.863	7.9	1.23	29.7
Acceleration (m/s <sup>2</sup> )	0.912	12.5	0.19	42.4
Speed (m/s)	0.99	3.1	0.61	47
Decelerated from 65 mi/h and maintained at 25 mi/h				
Gas pedal angle (°)	0.903	23.5	0.55	32.1
Acceleration (m/s <sup>2</sup> )	0.953	5	0.17	34.6
Speed (m/s)	0.993	3.7	0.46	60.7
Brake pedal angle (°)	0.936	9.1	2.54	44.2
Average of the percentage of improved $R^2$ and RMS		9.3		41.5

“Improved” means improved  $R^2$  and RMS from the Section IV-A.

TABLE IV  
 $R^2$  AND RMS FOR MODELED INDIVIDUAL SPEED

	Accelerated from 25 mi/h and maintained at 65 mi/h		Decelerated from 65 mi/h and maintained at 25 mi/h	
	$R^2$	RMS	$R^2$	RMS
Driver 1	0.997	0.376	0.982	0.782
Driver 2	0.965	1.157	0.982	0.749
Driver 3	0.962	1.052	0.986	0.701
Driver 4	0.99	0.543	0.957	1.053
Driver 5	0.993	0.541	0.709	2.782
Driver 6	0.974	1.049	0.994	0.456
Driver 7	0.947	1.325	0.991	0.577
Driver 8	0.761	3.111	0.952	1.155
Driver 9	0.981	0.78	0.97	0.908
Driver 10	0.977	1.024	0.954	1.205
Driver 11	0.947	1.567	0.945	1.312
Driver 12	0.972	0.967	0.964	0.936

the effects of both individual decision making references and impulsiveness, the model accounted for over 99% of the experimental speed of the average driver and over 95% of the experimental speed for the majority of individual drivers.

This paper is one of a few mathematical models with analytic solutions in the field of studying a driver’s speed control behavior, while the original QN-MHP or Adaptive Control of Thought-Rational (ACT-R; [39], [40]) relied on simulation to model human performance. In general, mathematical models with analytic solutions are always rigorous and parsimonious compared to simulation models. They rely on a set of math equations rather than a branch of codes to accurately quantify the phenomenon. In addition, math equations are easy to integrate and embed in systems for the purposes of application, whereas simulation may require the conversion of codes to different computer languages that others can use and interpret. Another advantage of this paper is that it can model individual differences that few existing studies are able to model.

Previous acceleration models (both car-following and free-flow models) focus on vehicle performance, while there have been no model predictions offered for human behaviors. Compared to these models, this paper provides predictions with regards not only to the vehicle speed and acceleration, but also to human speed choice, reaction time, foot movement time, etc. As a result, this model has the potential to guide researchers or engineers in their efforts to find weak links and

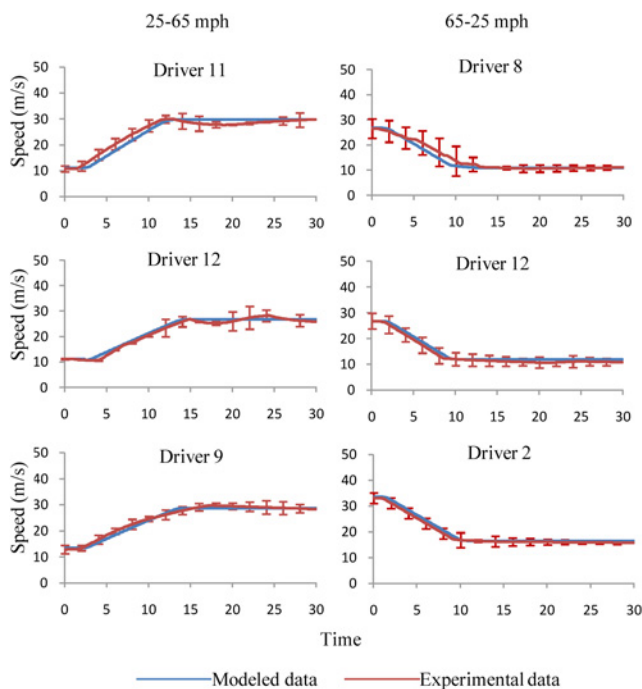


Fig. 3. Comparisons of modeled speed for individual driver with his/her experimental speed. From top to bottom: 1st, 2nd, and 3rd 4-quantiles for driving speed based on  $R^2$  results in an ascending order (error bars represent  $\pm 1$  standard deviation of experimental data).

bottlenecks in driver behavior and performance. Even though this paper models a driver's speed control behavior in free-flow driving settings, future work can extend and apply this model in a car-following or congested traffic condition (being extended). In such complex conditions, this model might switch from speed control mode (where the driver follows his/her desired target speed) to distance control mode (where the driver has to adjust distance/headway due to an obstacle ahead). This is also the way in which some advanced driving supporting systems work, such as Adaptive Cruise Control (ACC).

The major contribution of this paper was in expanding the original QN-MHP to model a driver's behavior of longitudinal vehicle control, indicating the potential application of QN-MHP in modeling integrated driving behaviors involving both lateral and longitudinal vehicle controls. Liu *et al.* [2] successfully employed QN-MHP to model driver performance of the lateral vehicle control, such as steering and lane keeping. In their paper, the authors also addressed the necessity of expanding the model of lateral vehicle control to include speed control so that the integrated driving behaviors could be well explained and predicted. The current model is built on the basis of the integration of QN-MHP and RDFT and all math equations proposed were implemented in corresponding servers of the QN-MHP. As a result, it is possible to integrate the current mathematical model of speed control with the existing cognitive modeling approach of lateral control to model integrated driving behaviors.

In addition, quantitative analyses and predictions with regard to a driver's profile and driving patterns can help transportation engineers/manufacturers better understand human

capabilities and the limitations of their speed control at an early stage of vehicle system design. For example, existing studies indicated that fuel consumption and emissions are particularly sensitive to changes in vehicle speed and acceleration [41]–[43]. Ahn [41] used a nonlinear multiple regression model and neural network techniques to approximate vehicle fuel consumption and emissions as a function of speed and acceleration. According to Ahn's model, the optimal fuel consumption can be calculated given a specific level of a vehicle's speed and acceleration. Therefore, if automobile engineers are capable of knowing a driver's profile and driving patterns as predicted by the current model, they can better design engine/transmission technologies and in-vehicle fuel efficient support tools [44]. Moreover, knowledge-driven components on road element characteristics are important for fuel-efficient driving. For example, if an experienced driver anticipates the presence of an intersection, he/she can adapt fuel-efficient driving strategies (e.g., step on the brake pedal early on and lightly [9]) to reduce fuel consumption. This model can also help engineers design a better electric vehicle (EV) battery for optimal discharge rate and battery lifetime. Previous research on EV batteries found that vehicle speed and acceleration had significant effects on battery lifetime [45]–[47]. If a driver's speed and acceleration can be predicted, the vehicle engineer can design a more effective EV battery management system (BMS) to manage a better charging strategy, or provide the driver appropriate feedback in order to prolong the lifetime of the EV battery.

The National Center for Statistics and Analysis [48] reported that speeding is a contributing factor in about one-third of all fatal traffic crashes in the United States and costs the country an estimated \$40 billion annually. In practice, the current model has value for predicting the occurrence of speeding and reducing the risk of speeding-related traffic accidents or injuries (being extended). The current findings ( $R^2$  and RMS results) showed that this model accounted for over 95% of experimental speed with small magnitudes of variation for the majority of individual drivers. This indicates that the model was able to predict the time at which a driver exceeds the speeding criterion (e.g., posted speed limit plus a small tolerance) and the magnitude of speeding. When speeding is detected, a warning message can be played to warn the driver about his/her current speed before speeding occurs. However, because this model considers the component of decision making, it can predict the occurrence of intentional speeding (i.e., the driver has the intention or motivation to change his/her speed given the internal/external stimulus). Future work could extend this model to predict the occurrence of unintentional speeding due to a lack of awareness of the current speed limit and/or traveling speed or inaccurate motor control.

Despite the conclusive findings of this paper, it is necessary to consider its limitations so that they may be addressed in the future. The model developed in this paper was validated via a driving simulator study, which may produce different speed perception and control for subjects compared with real-road driving. The main concern of using the driving simulator is that the mechanical model of a real car is proprietary. It is difficult to obtain the detailed expressions and parameters

TABLE V  
PARAMETER SETTINGS IN THE CURRENT MODEL

Parameter	Value (unit)	Description	Source
$K_1$	0.118–0.1232	The slope of the linear increase (in log–log space) of perceived speed with increasing texture density	[12], [13]
$P$	4%	The percentage of eye fixations performed on the speedometer	[8]
$\bar{T}_s$	760–880 (ms)	Eye fixation time spent on looking at the speedometer	[14]
$\theta$	1	Decision threshold in RDFT	[6]
$T_P$	126 (ms)	Visual information perception time	[2]
$T_B T_C T_F T_H$	18 (ms)	Processing time at Server B, C, F, and H	[2]
$T_W T_Y T_Z$	24 (ms)	Processing time at Server W, Y, and Z	[2]
$\lambda$	0.39	A constant sensitivity term that was used to estimate parameter A	[4]
$\eta$	0.736 (non-impulsive); 1 (normal driver); 1.533 (impulsive)	A term that represents the degree of impulsivity to act rapidly without deliberation	[30]
$A_l$	60 (mm)	Lateral separation of both pedals	Driving simulator
$A_p$	20 (mm)	Perpendicular separation of both pedals	Driving simulator
$B$	–0.64 (acceleration); –1.53 (deceleration)	The coefficient which represents the ratio of the deviation of the acceleration over the deviation of the pedal input	[22]
$c_g$	$10^-$	The coefficient of the overall drag on the vehicle	Driving simulator

for a real car. Also, the extreme complexity of the mechanical model (e.g., engine torque, transmission torque, braking torque, drivetrain load, aerodynamics, fiction, etc.) makes it difficult to quantify the relation between the pedal input and vehicle acceleration and speed. Therefore, the enhancement of the vehicle’s mechanical component and real road tests might be needed in future studies to validate this model. In addition, we briefly introduced how to extend the current work to model the effects of rule- or knowledge-driven components (e.g., road characteristics, weather condition; [49]) on a driver’s speed choice (see Section II-C2). For example, we can conduct a matrix to model the influence of curves on a driver’s speed choice, but we have to know the driver’s attitude toward speed choice at each level of curves/lane width (i.e., rules). This set of rules develops for each driver as he/she gains more driving experience, and begins to compete with his/her primary attributes listed in the main text (e.g., time benefit, monetary cost, safety gain) depending on the driver’s speed preference in any given situation. Due to page limits, however, it is extremely hard to model all of these aspects in one study and we are extending the model to consider these important topics in our future work.

#### APPENDIX A RDFT MATHEMATICAL DEDUCTION AND PARAMETERS ESTIMATION

First, each driver’s subjective attribute matrix (Table I) was converted into a normalized  $4 \times 4$  attribute matrix  $M'_{4 \times 4}$ . The

attention weights matrix  $W(t)$  was assumed to select only a single attribute  $j$  from  $M$  at each point in time during deliberation [6] for an average driver or normal drivers. In this case,  $W(t)$  was equal to 1 if  $j$  was selected, and 0 if  $j$  was not selected. For those drivers who are characterized as impulsive or non-impulsive,  $W(t)$  was set based on the probability of attention to each attribute.

The contrast matrix  $C$  was set as its default form: the diagonal elements  $C_{xx} = 1$  and the off-diagonal elements  $C_{xy} = -1/(m - 1)$ , where  $m$  is the number of alternatives ( $m = 4$  in present study)

$$C = \begin{bmatrix} 1 & -0.33 & -0.33 & -0.33 \\ -0.33 & 1 & -0.33 & -0.33 \\ -0.33 & -0.33 & 1 & -0.33 \\ -0.33 & -0.33 & -0.33 & 1 \end{bmatrix}.$$

The feedback matrix  $S$  was also set following the previous work [15]: the diagonal elements  $S_{xx} = 1$  and the off-diagonal elements  $S_{xy}$  were equal to a small nonzero number ( $S_{xy} = -0.001$  in this case) which accounts for a wide range of robust empirical phenomena

$$S = \begin{bmatrix} 0.95 & -0.001 & -0.001 & -0.001 \\ -0.001 & 0.95 & -0.001 & -0.001 \\ -0.001 & -0.001 & 0.95 & -0.001 \\ -0.001 & -0.001 & -0.001 & 0.95 \end{bmatrix}.$$

Finally, the threshold parameter  $\theta$  was used to determine when a driver’s speed choice is made. Regardless of the effect of personal characteristics,  $\theta$  was set equal to 1 which is a

$$M_{4 \times 4} = \begin{bmatrix} 100 & 100 & 100 & 100 \\ -300 & 250 & 250 & 250 \\ -250 & -300 & 500 & 500 \\ -500 & -300 & -300 & 750 \end{bmatrix} \rightarrow M'_{4 \times 4} = \begin{bmatrix} 1.35 & 0.58 & -0.11 & -1.05 \\ -0.25 & 1.11 & 0.34 & -0.52 \\ -0.05 & -0.85 & 1.08 & 0.35 \\ -1.05 & -0.85 & -1.31 & 1.22 \end{bmatrix}$$

moderately low level of overall preference necessary to make a speed choice [6]. With the parameter specification given, 1000 replications of the simulations were conducted in MATLAB for each driver. Each replication represents a new encounter of the decision making (determining a target speed).

APPENDIX B

VEHICLE MECHANICAL MODEL MATH DEDUCTION AND PARAMETERS ESTIMATION

Based on (9), the deviation of the pedal angle at each short time interval  $\Delta t$  was expressed as follows

$$d\theta = \int_0^{\Delta t} A \times \eta \times (v_{tar}^* - v_p) \times dt. \quad (15)$$

By combining (11) with (15), the deviation of acceleration at each short time interval  $\Delta t$  was

$$da = \int_0^{\Delta t} A \times B \times \eta \times (v_{tar}^* - v_p) \times dt. \quad (16)$$

Ahmed [4] developed a free-flow acceleration model in which the driver had the freedom to attain his/her desired speed without the effects of surrounding traffic. As introduced above, the term  $\lambda$  describes the difference between the driver's desired speed and the current speed at time  $t$ , and  $\lambda$  refers to a constant sensitivity term ( $\lambda=0.39$ ). In this proposed work,  $A \times B$  represented a similar sensitivity term. Because the parameter  $B$  was directly obtained from the STISIM driving simulator, the parameter  $A$  was computed accordingly.

According to (12) and (16), the acceleration applied by the driver at the time  $(t + \Delta t)$  was described in (17). Note that the acceleration inversely varies with the vehicle mass, assuming that the composition of forces exerted on the vehicle remains constant

$$a = a_0 - a_g + \int_0^{\Delta t} A \times B \times \eta \times (v_{tar}^* - v_p) \times dt. \quad (17)$$

Finally, the vehicle speed at the next time interval was

$$V = V_0 + [a_0 - a_g + \int_0^{\Delta t} A \times B \times \eta \times (v_{tar}^* - v_p) \times dt] \times \Delta t. \quad (18)$$

APPENDIX C

SETTING OF PARAMETERS IN THE CURRENT MODEL

Model parameters were set based on either existing studies or the STISIM driving simulator (Table V).

ACKNOWLEDGMENT

The authors would like to thank the anonymous reviewers for their valuable comments to improve this paper.

REFERENCES

[1] J. I. Elkind, S. K. Card, J. Hochberg *et al.*, *Human Performance Models for Computer-Aided Engineering*, Washington, DC, USA: National Academy Press, 1989.

[2] Y. Liu, R. Feyen, and O. Tsimhoni, "Queuing Network-Model Human Processor (QN-MHP): A computational architecture for multitask performance in human-machine systems," *ACM Trans. Comput.-Hum. Interact. (TOCHI)*, vol. 13, no. 1, pp. 37-70, Mar. 2006.

[3] R. E. Chandler, R. Herman, and E. W. Montroll, "Traffic dynamics: Studies in car following," *Oper. Res.*, vol. 6, no. 2, pp. 165-184, Mar.-Apr. 1958.

[4] K. I. Ahmed, "Modeling drivers' acceleration and lane changing behavior," Department of Civil and Environmental Engineering, Massachusetts Institute of Technology, Cambridge, MA, USA, Jan. 1999.

[5] T. Toledo, H. N. Koutsopoulos, and M. Ben-Akiva, "Integrated driving behavior modeling," *Transport. Res. C, Emerg. Technol.*, vol. 15, no. 2, pp. 96-112, Apr. 2007.

[6] J. G. Johnson and J. R. Busemeyer, "Rule-based Decision Field Theory: A dynamic computational model of transitions among decision-making strategies," in *The Routines of Decision Making*, T. Betsch and S. Haberstroh, Eds., pp. 3-20, Mahwah, NJ, USA: Lawrence Erlbaum, 2005.

[7] J. R. Busemeyer and J. T. Townsend, "Decision field theory: A dynamic-cognitive approach to decision making in an uncertain environment," *Psychol. Rev.*, vol. 100, no. 3, pp. 432-459, Jul. 1993.

[8] M. A. Recarte and L. M. Nunes, "Effects of verbal and spatial-imagery tasks on eye fixations while driving," *J. Exp. Psychol., Appl.*, vol. 6, no. 1, pp. 31-43, Mar. 2000.

[9] C. Wu, G. Zhao, and B. Ou, "A fuel economy optimization system with applications in vehicles with human drivers and autonomous vehicles," *Transp. Res. D: Transport Environ.*, vol. 16, no. 7, pp. 515-524, Oct. 2011.

[10] M. A. Recarte and L. M. Nunes, "Perception of speed in an automobile: Estimation and production," *J. Exp. Psychol., Appl.*, vol. 2, no. 4, pp. 291-304, Dec. 1996.

[11] D. H. Owen, L. Wolpert, and R. Warren, "Effects of optical flow acceleration, edge acceleration, and viewing time on the perception of egospeed acceleration," in *Optical Flow and Texture Variables Useful in Detecting Decelerating and Accelerating Self-Motion*, D. H. Owen, Ed., pp. 79-133, Williams Air Force Base, AZ: Air Force Human Resources Laboratory, 1984.

[12] B. P. Dyre and G. J. Andersen, "Image velocity magnitudes and perception of heading," *J. Exp. Psychol., Hum. Percept. Perform.*, vol. 23, no. 2, pp. 546-565, Apr. 1997.

[13] S. N. J. Watamaniuk, N. M. Grzywacz, and A. L. Yuille, "Dependence of speed and direction perception on cinematogram dot density," *Vis. Res.*, vol. 33, no. 5-6, pp. 849-859, Mar.-Apr. 1993.

[14] R. R. Mourant and T. H. Rockwell, "Strategies of visual search by novice and experienced drivers," *Hum. Factors, J. Hum. Factors Ergon Soc.*, vol. 14, no. 4, pp. 325-335, Aug. 1972.

[15] R. M. Roe, J. R. Busemeyer, and J. T. Townsend, "Multialternative decision field theory: A dynamic connectionist model of decision making," *Psychol. Rev.*, vol. 108, no. 2, pp. 370-392, Apr. 2001.

[16] B. Lin and C. Wu, "Mathematical modeling of the human cognitive system in two serial processing stages with its applications in adaptive workload-management systems," *IEEE Trans. Intell. Transp. Syst.*, vol. 12, no. 1, pp. 221-231, Mar. 2011.

[17] E. R. Hoffmann, "A comparison of hand and foot movement times," *Ergonomics*, vol. 34, no. 4, pp. 397-406, 1991.

[18] E. R. Hoffmann and K. C. Gan, "Directional ballistic movement with transported mass," *Ergonomics*, vol. 31, no. 5, pp. 841-856, 1988.

[19] M. Porter and D. E. DYI, "Exploring the optimum posture for driver comfort," *Int. J. Vehicle Des.*, vol. 19, no. 3, pp. 255-266, May 1998.

[20] E. R. Hoffmann, "Accelerator-to-brake movement times," *Ergonomics*, vol. 34, no. 3, pp. 277-287, 1991.

[21] P. Ioannou and Z. Xu, "Throttle and brake control systems for automatic vehicle following," *J. Intell. Transport. Syst.*, vol. 1, no. 4, pp. 345-377, Apr. 1994.

[22] G. Zhao, C. Wu, R. J. Houston *et al.*, "The effects of binge drinking and socio-economic status on sober driving behavior," *Traffic Injury Prevention*, vol. 11, no. 4, pp. 342-352, Aug. 2010.

[23] D. Royal, "National survey of speeding and unsafe driving attitudes and behaviors: 2002. Volume II—Findings report," National Highway Traffic Safety Administration (NHTSA), Nov. 2003.

[24] D. M. Zaidel, "A modeling perspective on the culture of driving," *Accident Anal. Prev.*, vol. 24, no. 6, pp. 585-597, Dec. 1992.

[25] J. L. Deffenbacher, R. S. Lynch, L. B. Filetti *et al.*, "Anger, aggression, risky behavior, and crash-related outcomes in three groups of drivers," *Behav. Res. Ther.*, vol. 41, no. 3, pp. 333-349, Mar. 2003.

- [26] E. R. Dahlen, R. C. Martin, K. Ragan *et al.*, "Driving anger, sensation seeking, impulsiveness, and boredom proneness in the prediction of unsafe driving," *Accident Anal. Prev.*, vol. 37, no. 2, pp. 341–348, Mar. 2005.
- [27] E. S. Barratt, "Impulsiveness and aggression," in *Violence and Mental Disorder: Developments in Risk Assessment*, J. Monahan and H. J. Steadman, Eds., pp. 61–79, Chicago, USA: University of Chicago Press, 1994.
- [28] H. J. Eysenck and S. B. G. Eysenck, *Manual of the Eysenck Personality Questionnaire*, San Diego, CA, USA: Educational and Industrial Testing Service, 1975.
- [29] S. B. G. Eysenck, H. J. Eysenck, and P. Barrett, "A revised version of the psychoticism scale," *Pers. Individ. Differ.*, vol. 6, no. 1, pp. 21–29, 1985.
- [30] J. A. Bachorowski and J. P. Newman, "Impulsive motor behavior: Effects of personality and goal salience," *J. Pers. Soc. Psychol.*, vol. 58, no. 3, pp. 512–518, Mar. 1990.
- [31] J. A. Gray, "A critique of Eysenck's theory of personality," in *A Model for Personality*, H. J. Eysenck, Ed., pp. 246–276, Berlin, Germany: Springer-Verlag, 1981.
- [32] D. C. Fowles, "The three arousal model: Implications of Gray's two factor learning theory for heart rate, electrodermal activity, and psychopathology," *Psychophysiology*, vol. 17, no. 2, pp. 87–104, Mar. 1980.
- [33] S. L. Nichols and J. P. Newman, "Effects of punishment on response latency in extraverts," *J. Pers. Soc. Psychol.*, vol. 50, no. 3, pp. 624–630, Mar. 1986.
- [34] A. D. Pickering and J. A. Gray, "The neuroscience of personality," in *Handbook of Personality: Theory and research*, L. A. Pervin and O. P. John, Eds., pp. 277–299, New York, NY, USA: Guilford Press, 1999.
- [35] Transportation Research Board, "Highway Capacity Manual," Washington, DC: National Research Council, 2000.
- [36] B. E. John, "Contributions to engineering models of human-computer interaction," Department of Psychology, Carnegie-Mellon University, Pittsburgh, PA, USA, 1988.
- [37] B. E. John, "TYPDIST: A theory of performance in skilled typing," *Hum.-Comput. Interaction*, vol. 11, no. 4, pp. 321–355, 1996.
- [38] C. Wu and Y. Liu, "Queuing network modeling of transcription typing," *ACM Trans. Comput.-Hum. Interact. (TOCHI)*, vol. 15, no. 1, Article 6, pp. 1–45, May 2008.
- [39] D. D. Salvucci, "Modeling driver behavior in a cognitive architecture," *Hum. Factors, J. Hum. Factors Ergon. Soc.*, vol. 48, no. 2, pp. 362–380, 2006.
- [40] D. D. Salvucci, and J. Beltowska, "Effects of memory rehearsal on driver performance: Experiment and theoretical account," *Hum. Factors, J. Hum. Factors Ergon. Soc.*, vol. 50, no. 5, pp. 834–844, Oct. 2008.
- [41] K. Ahn, "Microscopic fuel consumption and emission modeling," Civil and Environmental Engineering, Virginia Polytechnic Institute and State University, Blacksburg, VA, USA, Dec. 1998.
- [42] E. Ericsson, "Independent driving pattern factors and their influence on fuel-use and exhaust emission factors," *Transport. Res. D, Transport. Environ.*, vol. 6, no. 5, pp. 325–345, Sep. 2001.
- [43] R. Jourard, P. Jost, J. Hickman *et al.*, "Hot passenger car emissions modelling as a function of instantaneous speed and acceleration," *Sci. Total Environ.*, vol. 169, no. 1–3, pp. 167–174, Jul. 1995.
- [44] M. van der Voort, M. S. Dougherty, and M. van Maarseveen, "A prototype fuel-efficiency support tool," *Transport. Res. C*, vol. 9, no. 4, pp. 279–296, 2001.
- [45] A. Mills and S. Al-Hallaj, "Simulation of passive thermal management system for lithium-ion battery packs," *J. Power Sources*, vol. 141, no. 2, pp. 307–315, Mar. 2005.
- [46] A. A. Pesaran, "Battery thermal management in EVs and HEVs: Issues and solutions," in *Proc. Advanced Automotive Battery Conf.*, Las Vegas, NV, USA, Feb. 6–8, 2001.

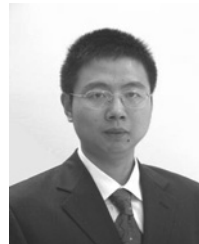
- [47] P. Ramadass, B. Haran, R. White *et al.*, "Capacity fade of Sony 18650 cells cycled at elevated temperatures: Part I. Cycling performance," *J. Power Sources*, vol. 112, no. 2, pp. 606–613, Nov. 2002.
- [48] NCSA, "Traffic safety facts: Speeding," Dept. of Transportation, Nat. Center Statist. Anal., Washington, DC, USA, 2004.
- [49] W. Van Winsum and H. Godthelp, "Speed choice and steering behavior in curve driving," *Hum. Factors, J. Hum. Factors and Ergon. Soc.*, vol. 38, no. 3, pp. 434–441, Sep. 1996.



**Guozhen Zhao** received the B.S. degree in industrial engineering, from Tianjin University, China, in 2007, and the M.S. and Ph.D. degrees in industrial and systems engineering from the State University of New York, Buffalo, NY, USA, in 2009 and 2011, respectively.

He is the author of published papers in *Journal of Power Sources*, *Accident Analysis & Prevention*, *Transportation Research Part D: Transport and Environment*, *Behaviour & Information Technology*, *Traffic Injury Prevention*, *The International Journal of Industrial Ergonomics*. His current research interests include the mathematical modeling of human cognition and performance, transportation safety, human computer interaction, and neuroergonomics and their applications in intelligent system design.

Dr. Zhao is a member of a Human Factors and Ergonomics Society. He has been a reviewer for the IEEE TRANSACTION ON INTELLIGENT TRANSPORTATION SYSTEM, IEEE TRANSACTIONS ON SYSTEMS, MAN, AND CYBERNETICS PART A: SYSTEMS AND HUMANS, and Applied Ergonomics.



**Changxu Wu** (S'04–M'07) received the B.S. degree in psychology, focusing on engineering and mathematical psychology, from Zhejiang University, Hangzhou, China, in 1999, the M.S. degree in engineering psychology and human-computer interaction from the Chinese Academy of Sciences, Beijing, China, in 2002, and the M.S. and Ph.D. degrees in industrial and operational engineering from the University of Michigan, Ann Arbor, MI, USA, in 2004 and 2007, respectively.

Since August 2007, he has been an Assistant Professor with the Department of Industrial and System Engineering, State University of New York, Buffalo. His current research interests include the development of computational models of human performance and mental workload, addressing both the fundamental and neurological issues of perceptual-motor behavior and human cognition with their applications in designing intelligent transportation systems.

Dr. Wu is currently an Associate Editor of two leading journals in human factors domain: IEEE TRANSACTIONS ON INTELLIGENT TRANSPORTATION SYSTEMS and *Behavior and Information Technology*. He has published 31 journal papers in human factors, psychology, and human-computer interaction, including *Psychological Review*, *ACM Transactions on Computer-Human Interaction*, IEEE TRANSACTIONS ON SYSTEMS, MAN AND CYBERNETICS, IEEE TRANSACTIONS ON INTELLIGENT TRANSPORTATION SYSTEMS, *International Journal of Human-Computer Studies*, and *Ergonomics*. He was a recipient of the Outstanding Student Instructor Award from the American Society of Engineering Education at the University of Michigan in 2006.